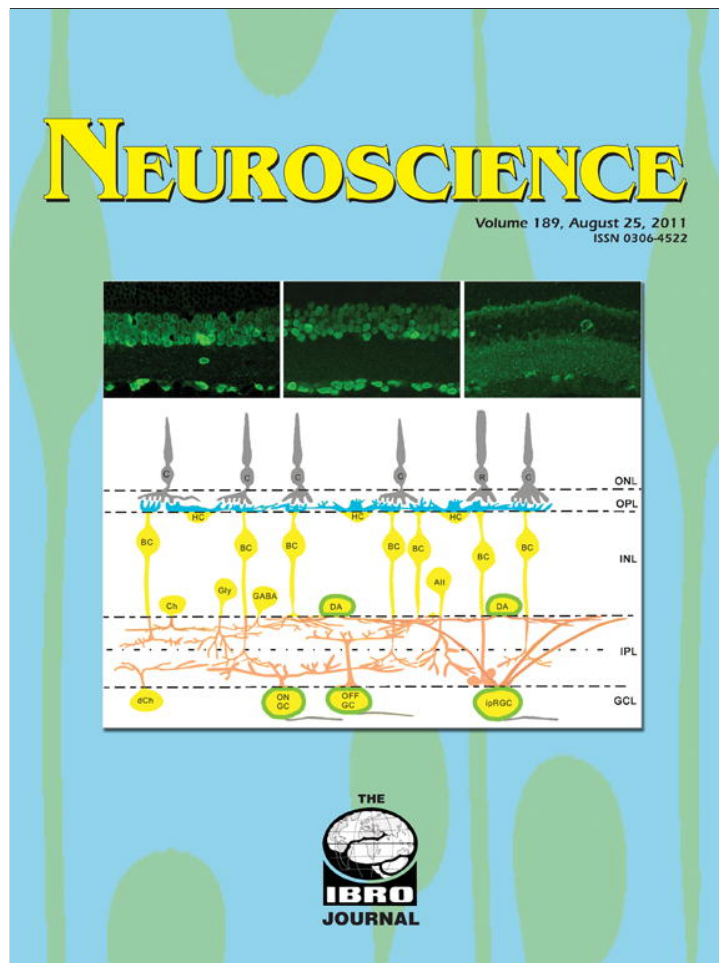


Provided for non-commercial research and education use.
Not for reproduction, distribution or commercial use.



This article appeared in a journal published by Elsevier. The attached copy is furnished to the author for internal non-commercial research and education use, including for instruction at the authors institution and sharing with colleagues.

Other uses, including reproduction and distribution, or selling or licensing copies, or posting to personal, institutional or third party websites are prohibited.

In most cases authors are permitted to post their version of the article (e.g. in Word or Tex form) to their personal website or institutional repository. Authors requiring further information regarding Elsevier's archiving and manuscript policies are encouraged to visit:

<http://www.elsevier.com/copyright>

GRIP FORCE REGULATES HAND IMPEDANCE TO OPTIMIZE OBJECT STABILITY IN HIGH IMPACT LOADS

O. WHITE,^{a,b,c,d,*} J.-L. THONNARD,^c A. M. WING,^e
R. M. BRACEWELL,^d J. DIEDRICHSEN^{d,f} AND
P. LEFÈVRE^{c,g}

^aUniversité de Bourgogne, Campus Universitaire, Unité de Formation et de Recherche en Sciences et Techniques des Activités Physiques et Sportives, BP 27877, F-21078 Dijon, France

^bInstitut National de la Santé et de la Recherche Médicale, Unité 887, Motricité-Plasticité, Dijon, France

^cInstitute of Neuroscience (IoNS), Université catholique de Louvain, 4 Avenue Georges Lemaître, 1348 Louvain-la-Neuve, Belgium

^dWolfson Centre for Clinical and Cognitive Neuroscience, Adeilad Brigantia, Bangor University, Gwynedd LL57 2AS, UK

^eSensorimotor Neuroscience (SyMoN), Behavioural Brain Sciences, School of Psychology, University of Birmingham, Edgbaston, Birmingham, B15 2TT, UK

^fInstitute of Cognitive Neuroscience, University College London, Alexandra House, 17 Queen Square, London WC1N 3AR, UK

^gICTEAM Institute, Université catholique de Louvain, 4 Avenue Georges Lemaître, 1348 Louvain-la-Neuve, Belgium

Abstract—Anticipatory grip force adjustments are a prime example of the predictive nature of motor control. An object held in precision grip is stabilized by fine adjustments of the grip force against changes in tangential load force arising from inertia during acceleration and deceleration. When an object is subject to sudden impact loads, prediction becomes critical as the time available for sensory feedback is very short. Here, we investigated the control of grip force when participants performed a targeted tapping task with a hand-held object. During the initial transport phase of the movement, load force varied smoothly with acceleration. In contrast, in the collision, load forces sharply increased to very large values. In the transport phase, grip force and load force were coupled in phase, as expected. However, in the collision, grip force did not parallel load force. Rather, it exhibited a stereotyped profile with maximum ~65 ms after peak load at contact. By using catch trials and a virtual environment, we demonstrate that this peak of grip force is pre-programmed. This observation is validated across experimental manipulations involving different target stiffness and directions of movement. We suggest that the central nervous system optimizes stability in object manipulation—as in catching—by regulating mechanical parameters including stiffness and damping through grip force. This study provides novel insights about how the brain coordinates grip force in manipulation involving an object interacting with the environment. © 2011 IBRO. Published by Elsevier Ltd. All rights reserved.

*Correspondence to: O. White, INSERM - U887 Motricité-Plasticité, Performance, Dysfonctionnement, Vieillesse et Technologies d'optimisation. Université de Bourgogne, UFR STAPS, Dijon, France. Fax: +33-3-80-39-67-02.

E-mail address: olivier.white@u-bourgogne.fr (O. White).

Abbreviations: GF, grip force; IREDs, infrared-light-emitting diodes.

0306-4522/11 \$ - see front matter © 2011 IBRO. Published by Elsevier Ltd. All rights reserved.

doi:10.1016/j.neuroscience.2011.04.055

Key words: reflex, load force, perturbation, stiffness, object manipulation.

When we move the hand while holding an object in precision grip, tangential load forces arising from inertia in accelerating and decelerating the object challenge the grip. Stabilization within the hand is ensured through anticipatory grip force adjustments (Flanagan et al., 1993; Flanagan and Wing, 1993, 1995; Wing, 1996). There is evidence for a systematic modulation of grip force with various changes in load force including those dependent on position, velocity and acceleration (see for example Flanagan and Wing, 1997; Nowak et al., 2004a).

A hand-held object may collide with other objects in the environment. In such cases the load increases very quickly, and prediction becomes more critical as the time available for sensory feedback is very short. Several studies have addressed the control of grip force in collision tasks (Johansson and Westling, 1988; Serrien et al., 1999; Nowak and Hermsdorfer, 2006). In particular, one investigation involved keeping a hand-held receptacle in position when a ball was dropped into it (Johansson and Westling, 1988). When the participant dropped the ball, an anticipatory rise in grip force prior to collision was followed by an increase in grip force after collision that was attributed to a reflex. In other studies, participants moved an object to generate an impact (Serrien et al., 1999; Turrell et al., 1999; Delevoeye-Turrell et al., 2003) which also elicited grip force peaks after the contact. In the above studies, the occurrence of a maximum of grip force after impact contrasts with the grip-load force coupling when forces vary smoothly, where zero-delay between grip and load force maxima is observed.

The predictive nature of grip force mechanisms in tasks involving impulse-like forces has not been investigated in great detail. Recently, Bleyenheuft and colleagues (2009) asked participants to keep an object in a precision grip while an attached mass was dropped. After a series of such normal trials, participants still exhibited a peak of grip force after the *expected* impact in a blank trial (no actual drop occurred). An earlier study involved the transport of an object to impact a pendulum and cause it to swing (Turrell et al., 1999). In this latter study, the authors showed that participants were able to synchronize grip and load forces at impact if specific amplitude swings had to be generated. While these two studies show that grip force increases to impacts are predictive, they do not explain why peak grip force often occurs after impact.

Here we test the hypothesis that the delayed peak grip force with respect to an impact allows mainly the natural

damping properties of the skin to absorb high frequencies in the destabilizing forces to stabilize the grasp. In the first experiment, we asked participants to produce up and down collisions with two targets. We replicate the observation that maximal grip force occurs after the impact. We show that it remains true even when the transport of the object involves direction-dependent load force profiles. This indicates that two independent processes—one for the transport of the object and one for the collision with the target—are regulated to stabilize the grasp. In the second experiment, participants produced up collisions against stiff and soft targets in a virtual environment. Consistent with Experiment 1, we observed a delayed peak grip force after the impact for both targets. This new paradigm allowed us to implement catch trials in which the dynamic interaction with the target failed to occur on unpredictably selected trials. We could therefore clearly measure the predictive grip force component. Furthermore, we investigated whether the stiffness of the target modulates the latency of the grip force maximum. We hypothesize that the grip force profile should adapt as a function of stiffness in order to absorb the more pronounced dynamic transients when impacting a stiff surface.

EXPERIMENTAL PROCEDURES

In the first experiment, participants were instructed to tap a real target situated above or below the hand's neutral position with an instrumented object. In the second experiment, we asked another group of volunteers to produce collisions against a target while gripping a force transducer mounted on a robotic arm. We used a virtual environment to simulate stiff and soft targets and implemented catch trials in which the target was only presented visually.

Participants

Nine right-handed volunteers (22–48 years old, two females) participated in the first experiment and seven new participants (19–32 years old, one female) in the second experiment. All participants had normal or corrected to normal vision and did not report any motor disabilities. All participants gave their informed consent to participate in this study and the procedures were approved by the local ethics committees (Université catholique de Louvain, Belgium for Experiment 1 and School of Psychology, Bangor University, UK, for Experiment 2). They were naive as to the purpose of the experiments and were debriefed after the experimental session.

Experiment 1: up and down collisions with real targets

Equipment. The manipulandum comprised a cylindrical instrumented object (82 mm diameter, 30 mm wide, 212 g mass) equipped with two brass circular grip surfaces (40 mm diameter) mounted on two parallel lightweight force-torque sensors (Mini 40 F/T transducers, ATI Industrial Automation, NC, USA). The sensors measured the three force components (F_x , F_y , F_z) along the axes passing through the centre of the corresponding grasp surface. Sensing ranges for F_x , F_y and F_z were ± 40 , ± 40 and ± 120 N with 0.02, 0.02, and 0.06 N resolution respectively (White et al., 2008).

An OptoTrak 3020 system (Northern Digital, Ontario, Canada) tracked three infrared-light-emitting diodes (IREDs) on the manipulandum. The OptoTrak was mounted on the floor three meters

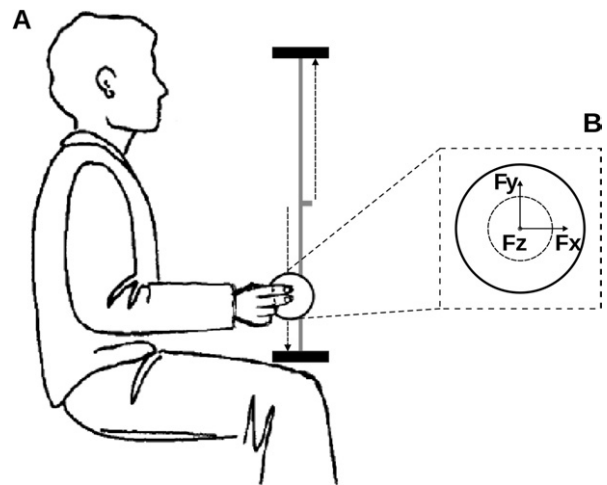


Fig. 1. (A) Lateral view of the experimental set-up used in Experiment 1. The participant produced collisions between the manipulandum (circle) and two targets (black rectangles). The horizontal elastic band (grey tick on the vertical line) was equidistant from the targets and defined the hand home position. (B) Scaled enlargement of the manipulandum (solid circle) with its 3-d reference frame centred on a sensor (dashed circle).

in front of the participant. The positions of the IREDs were aligned to a reference frame parallel to the floor. The X, Y and Z axes pointed rightward, upward and toward the participant, respectively. The positions of the three IREDs were sampled at a frequency of 200 Hz with a resolution of 0.1 mm.

A PXI controller (PXI-8156B) equipped with a 12-bit PXI-6071E A/D converter, external triggering facilities and an SCSI interface (PXI-8210, National Instruments, Austin, TX, USA) recorded the synchronized signals from the force sensors (1 kHz) and from the OptoTrak.

Procedure. The participant was comfortably seated on a chair. At a signal provided by the experimenter, the participant grasped the manipulandum between the thumb on one side and the index and middle fingers on the other side at about the centre of the grasp surfaces. The fingers were aligned so that the vertical force axes of the transducers (F_y) were aligned with the Y-axis of the reference frame (Fig. 1B). On each trial, participants moved the manipulandum from a home position up or down to tap an upper or lower target and then return back to the home position. No specific instructions were given regarding the velocity. The two circular targets (75 mm diameter), cushioned with 17 mm thick high density foam to limit the impact, were mounted 30 cm above and below the start position and parallel to the floor on two horizontal crossbars of a square frame (Fig. 1A). A red mark, vertically midway between the two targets, indicated the home position. A brief auditory tone prompted movement toward the upper (high tone) or lower (low tone) target. The tone onsets occurred at random between 300 and 500 ms after completion of the previous movement. Each participant performed five blocks of 40 randomized up and down collisions.

Data processing. The geometric centre of the manipulandum defined its position and was calculated from the three IREDs. Instantaneous velocity and acceleration were obtained using a 5-point central-difference algorithm. Hand movement onset was defined at the first sample at which the absolute velocity exceeded 0.15 m/s and remained above that threshold for at least 150 ms.

The force applied normally at each grasp surface was calculated as $-F_z$. The total normal grip force was calculated as the average of the normal forces applied by the thumb and the fingers on each transducer. The magnitude of the tangential load force

(LF) was computed as $LF = \sqrt{F_{x,1}^2 + F_{y,1}^2} + \sqrt{F_{x,2}^2 + F_{y,2}^2}$, where F_x and F_y are the horizontal and vertical components of the tangential force of each transducer. Therefore, in static condition, the load force equalled the object's weight (2.1 N). The impact force was obtained by averaging values of three samples centred on the maximum of load force.

All trials were aligned with the time of impact. We determined the values of grip force, load force and grip force rate at baseline, peak acceleration and 1 ms before target contact on the individual traces. The time of target contact was detected backward in time from the highest peak in load force. The grip force maximum and its time of occurrence were also measured. They corresponded to the maximum in grip force occurring at least 20 ms after the impact to avoid load force artefacts recorded on the Z-axis induced by small tilts off the vertical plane, as also observed in other studies (Nowak and Hermsdorfer, 2006). The position, velocity and acceleration signals were linearly interpolated to 1 kHz to match the sampling rate of the force signals.

Experiment 2: virtual soft and stiff collisions

Apparatus and stimuli. Participants were seated in front of a virtual environment with their head on a chin rest. A Nano-17 force-torque sensor (ATI Industrial Automation, NC, USA) was mounted at the end of a robotic device (Phantom 3.0, Sensable Technologies, RI, USA) to record grip force (normal force component, $-F_z$) and load force (tangential force components, F_x and F_y) at 1 kHz. Sensing ranges for F_x , F_y and F_z were ± 25 , ± 25 and ± 35 N with a 0.006-N resolution for the three axes. Participants looked into two mirrors that were mounted at 90 degrees to each other, such that they viewed one LCD screen with the right eye and one LCD screen with the left eye. This stereo display was calibrated such that the physical location of the robotic arm was consistent with the visual disparity information. Between trials, the position of the end-effector was represented as a small grey sphere (8 mm diameter).

The 3-d positions and forces of the robotic arm were controlled in closed loop at 1 kHz to simulate a spherical object (24 mm diameter, 212 g) held in the right hand. This object could be translated and rotated without constraint and was simulated using Newtonian rigid-body dynamics. To allow for the stable simulation of inertial objects, the endpoint of the robot was attached to the virtual object via a simulated spring (stiffness 800 N/m). The low-level routines of the robotic devices were rewritten, such that position and velocity were estimated using a Kalman filter. In this way, participants experienced the natural inertial and gravitational forces while manipulating the object in the workspace.

The targets were visually presented as coloured prisms ($120 \times 25 \times 30$ mm³) 150 mm above the start position. To simulate the target, the robot generated an elastic force field $F = k(y - h_0)$ when position exceeded a certain height (h_0) corresponding to the level of contact between the surfaces of the virtual object and the target prism. The stiff and soft targets were implemented with $k = 1200$ N/m and 240 N/m, respectively. This elastic force was added to the current inertial force experienced at contact.

Procedure. To initiate a trial, participants moved their right hand into a grey starting sphere (8 mm diameter), displayed at body midline and at chest height. Then, the grey weightless sphere was gradually morphed during 1000 ms into a 24-mm blue 212-g sphere to simulate the object. The target prism (red for stiff or green for soft) appeared 15 cm above the home position. Participants were instructed to move the object straight upward against the target prism and bring it back to the home position. To normalize the kinematics, participants adjusted the peak velocity of the object toward the target between 950 and 1050 mm/s. After each trial, a line was displayed at a height proportional to the peak velocity together with the lower (950 mm/s) and upper (1050

mm/s) bounds. The colour of the line was red if peak velocity was outside the interval or was green in successful trials.

The recording session comprised eight blocks of 40 collisions. The target condition (stiff or soft) alternated between blocks, and their order was counterbalanced between participants. In every block, eight trials (20%) were randomly chosen to be catch trials in which the elastic force field simulating the target vanished. In the remaining 32 trials, the natural object and target dynamics remained intact.

Data processing. The grip force was calculated as $-F_z$ and the magnitude of the tangential load force was computed as $LF = 2\sqrt{F_x^2 + F_y^2}$, where F_x and F_y are the horizontal and vertical components of the tangential force of the transducer. In static condition, the load force measured the simulated object's weight (2.1 N). As in Experiment 1, all trials were aligned to the time of impact and we determined the values of grip force and load force at baseline, peak acceleration, 1 ms before target contact, maximum of impact and maximum of grip force on the individual traces. The time of contact was measured when the position of the hand reached the height threshold (h_0).

Statistical analysis

In the two experiments, paired *t*-tests of individual subject means were used to investigate differences between blocks, direction (Experiment 1), type of trial (normal vs. catch) and target stiffness (Experiment 2) as the variables. The values reported in the text are mean \pm standard deviations. The statistical analysis was done using the SPSS package (SPSS Inc., Chicago, IL, USA) and Matlab.

RESULTS

In the first experiment, participants produced collisions with an object against two identical targets, situated 30 cm above or below the object's neutral position. We measured the grip force profiles en route to the target and at the collision to investigate the strategy to cope with impulse-like load forces.

Fig. 2 illustrates upward (left column, Up) and downward (right column, Down) trials for the same participant. In the upward collision, the vertical position increased until the manipulandum came into contact with the target (at time = 0 ms) and then decreased about 100 ms after contact to return to the starting position. Velocity exhibited a bell-shaped profile (max around 1.5 m/s), truncated at target contact. In the collision, velocity dropped sharply to zero and was briefly negative indicating a cycle of compression and decompression of the high density foam cushioning on the target. After hand movement onset (mean 306 ± 39 ms before contact across participants), the acceleration reached a maximum and then decreased to negative values. At collision, the acceleration exhibited a large negative value reflecting the nearly instantaneous drop of velocity and the spring-like interaction with the target. Before target contact, the load force was proportional to acceleration. At collision, the load force increased sharply up to a value around 15 N. After the initial phase of the movement where the grip force followed the load force profile, grip force increased up to a large peak on average 55.5 ± 19.5 ms after the impact, across all subjects.

In down collisions, velocity, acceleration and load force profiles matched those for the up collisions but in the

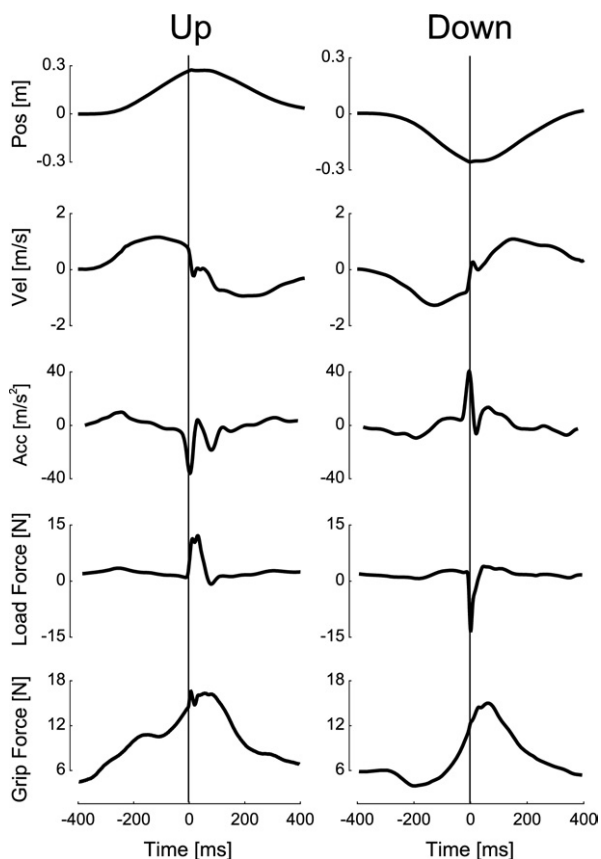


Fig. 2. Records of a single collision upwards (left column) and downwards (right column) from the same participant. The following traces are shown as a function of time: the vertical position, velocity and acceleration of the object, load force and grip force. The vertical line is positioned at target contact.

opposite direction. In contrast, grip force first exhibited a small depression that matched the early component of load force before increasing continuously prior to impact to reach a maximum 68.3 ± 17.4 after impact, for all participants.

These two representative trials show that in order to secure the object within the grasp, participants had to counteract inertial forces arising from the *transport* of the manipulandum, where a good correlation was observed between grip and load forces at peak acceleration ($r=0.55$, $P>0.001$, both directions), and then, had to cope with the very large perturbation forces at *collision*. The former are relatively low forces spanning over a moderately long period of time whereas the latter have impulse characteristics with large amplitude and short duration.

Fig. 3 depicts the mean load force (Fig. 3A) and grip force (Fig. 3B) in up and down trials at baseline (grey bars) and peak acceleration (white bars). Hatched bars report mean load force at impact and black bars represent mean grip force 1 ms before contact. At baseline, the load force was corresponded to the object's weight and was the same across directions (Fig. 3A, grey bars, $t_8 = -0.7$; $P=0.5$). Grip force baselines were also equivalent in up and down trials (Fig. 3B; grey bars, $t_8 = 0.6$; $P=0.571$). When the

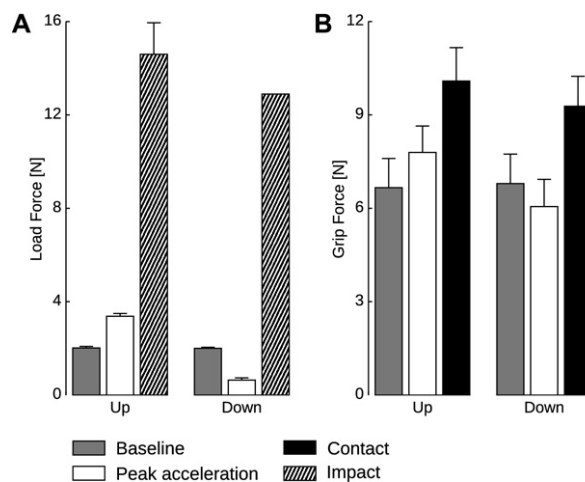


Fig. 3. Mean load force (A) and grip force (B) at baseline (grey bars), peak acceleration (white bars), contact (black bars) and impact (hatched bars) in upward (Up) and downward (Down) trials. Error bars represent SE across participants ($n=9$). Note the different Y-axis scales.

object was accelerated to the target, the inertial term added to or subtracted from the gravitational term, for up and down trials, respectively. Therefore, at peak acceleration, we measured larger load forces upwards compared to downwards (Fig. 3A, white bars, $t_8 = -15$; $P<0.001$). Participants adjusted grip forces accordingly, as evidenced by the larger grip forces upwards occurring at peak acceleration (Fig. 3B, white bars, $t_8 = -5$; $P=0.001$). This difference was also observed just before contact (Fig. 3B, black bars, $t_8 = -3$; $P=0.003$). In the up trials, grip force increased from baseline to peak acceleration and decreased in down trials. Impact forces were roughly matched (Fig. 3A, hashed bars, $t_8 = -2$; $P=0.089$).

We observed a maximum in grip force occurring at the same latency after impact in both directions (61.9 ± 19.1 ms, $t_8 = 1.5$; $P=0.184$). Within-subject trial-to-trial variability of the time to peak grip force in upward and downward collisions were similar (32.8 ms, $t_8 = 1$; $P=0.927$). We therefore proposed that this maximum in grip force might be pre-programmed. Interestingly, the load force at impact ($SD=6.2$ N) did not contribute significantly to predict the grip force maximum (correlation between grip force max and load force at impact, $P>0.05$). We then used a multiple regression to determine the correlation of grip force maximum (GF_M) with the grip force (GF_C) and its first derivative both prior to contact (dGF_C/dt), averaged across directions:

$$GM_M = 0.72GF_C + 0.05 \frac{dGF_C}{dt} + 0.92 \quad (1)$$

We found that the grip force maximum was significantly predicted by two variables calculated before contact (partial $R=0.95$ for GF_C and 0.84 for dGF_C/dt , both $P<0.001$). Both the values of grip force before contact and its slope contributed to predict the peak, which therefore rules out a pure short latency reflex mechanism. In sum, we found indirect evidence that this peak grip force was pre-pro-

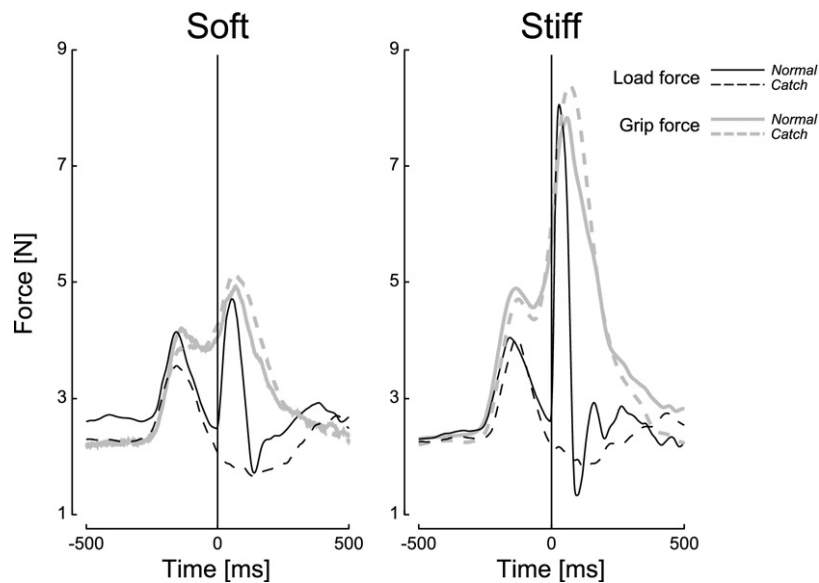


Fig. 4. Averaged load force (black lines) and grip force (grey lines) traces over time from one participant in normal (solid) and catch (dashed) trials during collisions with the soft (left panel) and the stiff (right panel) targets. The vertical line is positioned at target contact (0 ms). Catch and normal trials are very similar for the grip force profiles.

grammed and that it occurred at a fixed latency, independently of the movement direction.

Before discussing these findings, we turn to Experiment 2 to address two limitations of the first experiment that might challenge the pre-programming interpretation of the grip force profile after the impact. First, in the Experiment 1, all trials involved collisions with the targets. Therefore, we could not identify the predictive component of the grip force per se, but rather had to infer the proportion of pre-programmed vs. reactive grip force control using a mathematical model. In the second experiment, we addressed this issue by inserting 20% catch trials, in which the target was only visually presented and could be traversed without any resistance. With these trials, we were able to unambiguously interpret the grip force observed between contact and 100 ms after contact as pre-programmed by the motor system. Secondly, we thought to test one idea about the reason why the motor system pre-programs the maximal grip force after the collision, rather than simultaneously with it. We hypothesized that the grip force maximum is delayed with respect to the impact to damp high frequencies in the destabilizing forces occurring after impact. If this holds, the grip force profile should adapt as a function of stiffness in order to absorb the more pronounced dynamic transients when impacting a stiff surface.

Fig. 4 shows the average load force (black line) and grip force (grey line) in normal (solid) and catch (dashed) trials during collisions against the soft (left panel) and stiff (right panel) targets for one participant. As in Experiment 1, grip and load forces closely matched in the transport phase for both target stiffness ($r=0.96$, $P<0.001$). The vertical black line is positioned at contact, that is where the elastic forces were active to simulate the interaction with the target. In normal trials, the load force trace was similar

across targets before contact but reached larger peaks ($t_6=-4.1$; $P=0.009$) and in a shorter amount of time ($t_6=9.7$; $P<0.001$) in the stiff trials. Although participants produced similar kinematics before contact (same peak velocity en route to the target, 959 ± 9 mm/s, $t_6=0.7$; $P=0.486$), they expected a stronger impact in stiff trials, as evidenced by steeper grip force traces before contact. In agreement with Experiment 1, a grip force maximum was also observed 60.4 ± 15 ms after the contact, with no difference across targets ($t_6=1.3$; $P=0.252$).

To test the possibility that an additional reactive GF response was superimposed on the predictive component, we ran a factorial 2-way ANOVA with factors stiffness and trial type on grip force peaks. The type of trial did not influence the grip force peak ($F_{(1,24)}=0.04$, $P=0.835$) and we didn't find an interaction between trial type and stiffness ($F_{(1,24)}=0$, $P=0.959$).

Are peak grip forces more delayed after contact in stiff collisions than in soft collisions? This would allow for a more efficient damping of larger instabilities occurring in stiff trials. To test this, we reported the times of impact and the times of peak grip force (with respect to time of contact) in Experiment 1 (Up vs. Down) and in Experiment 2 (Stiff vs. Soft). Fig. 5 shows that the latency of maximum load force (triangles) almost doubled between stiff and soft trials (Experiment 2, 29.4 ms to 56.6 ms, $t_6=9.7$; $P<0.001$). It also shows that the latency of maximum grip force (black disks) relative to contact was the same across all experimental conditions (Experiment 1, up vs. down: $t_8=1.5$, $P=0.184$; Experiment 2, soft vs. stiff: $t_6=0.931$, $P=0.395$), including catch trials (grey disks, Experiment 2, normal vs. catch: $t_6=0.946$, $P=0.388$). Finally no difference was observed between experiments ($t_{12}=-0.063$, $P=0.951$).

Why does the grip force peak ~ 60 ms after target contact in all conditions? High frequencies in the force

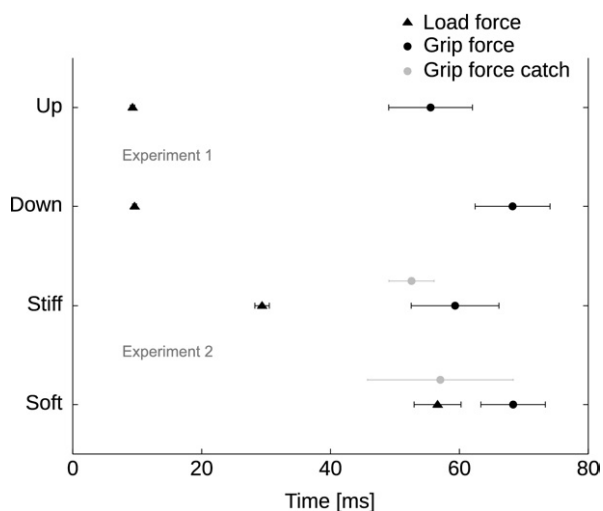


Fig. 5. Mean time occurrences of peak load force at impact (triangles) and peak grip force (black discs) across Experiment 1 (Up and Down) and Experiment 2 (Stiff and Soft). In Experiment 2, times of peak grip forces in catch trials are shown in grey. Error bars represent SE across participants.

signal can easily be damped out if the contact between the object and the fingers is loose. In contrast, destabilizing vibrations are sustained if the grasp interface is stiff. The mechanical rationale to desynchronize the peak of grip force from the peak of load force is simple: maximize the absorbed energy while ensuring stability after contact. Fig. 6A illustrates the accumulated mechanical constraints as measured by the integral of absolute load force from time of contact (0 ms) up to 100 ms in Soft (dashed curve) and Stiff (solid curve) trials. The first load force burst (main impact component) spanned over 63 ms on average (both experiments) and was significantly shorter than 100 ms ($t_{12} = -10.1$, $P < 0.001$). The 100-ms threshold therefore marks a reduction of the increase of the integral. The solid and dashed vertical lines in Fig. 6A are positioned at the mean occurrences of grip force peaks in Stiff and Soft

trials, respectively. The proportion of destabilizing load force absorbed up to maximum of grip force was 76.3% in the Stiff and 68.7% in the Soft trials (both $> 50\%$, $t_{11} = 63.5$, $P < 0.001$, 100% corresponds to the value of integral at 100 ms). The mean proportion of load force absorbed for the two collapsed stiffness conditions was 72.5%.

We conducted the same analysis on the data from Experiment 1 and partitioned the set according to impact amplitude (Fig. 6B, low impacts $<$ median 13 N; high impacts $>$ median 13 N). In line with Experiment 2, we found that the proportion of load force absorbed up to maximum of grip force was 77.6% in the high-impact trials and 69% in the low-impact trials (both $> 50\%$, $t_{17} = 38.7$, $P < 0.001$). The mean proportion of load force absorbed for the two collapsed conditions was 73.3%.

Interestingly, we also showed that the accumulated constraints were higher when the hand was stiffer in Experiment 1. Fig. 6C shows larger integral of load force up to 100 ms in trials when grip forces before contact are larger than the median grip force before contact ($t_8 = -2.6$; $P = 0.043$, 16% increase). This result cannot be explained by differences in impacts between the two sets of data since there was no difference in impact intensity between low- and high-grip force trials ($t_8 = -1.7$; $P = 0.131$). In addition, we expected a continuum between hand stiffness as measured through grip force before contact and ability to damp out transients as measured by integral load force. We indeed found a correlation between grip force before contact and integral ($r = 0.62$, $P < 0.001$) but not between grip force before contact and impact load force ($P = 0.252$).

To summarize, Experiment 2 confirmed and extended the observations made in Experiment 1. First, the grip force maximum was time-locked after the contact with the target, even when no real impact occurred in catch trials. This latency was compatible with the value reported in Experiment 1 which involved a different paradigm with different targets, directions of movements and participants.

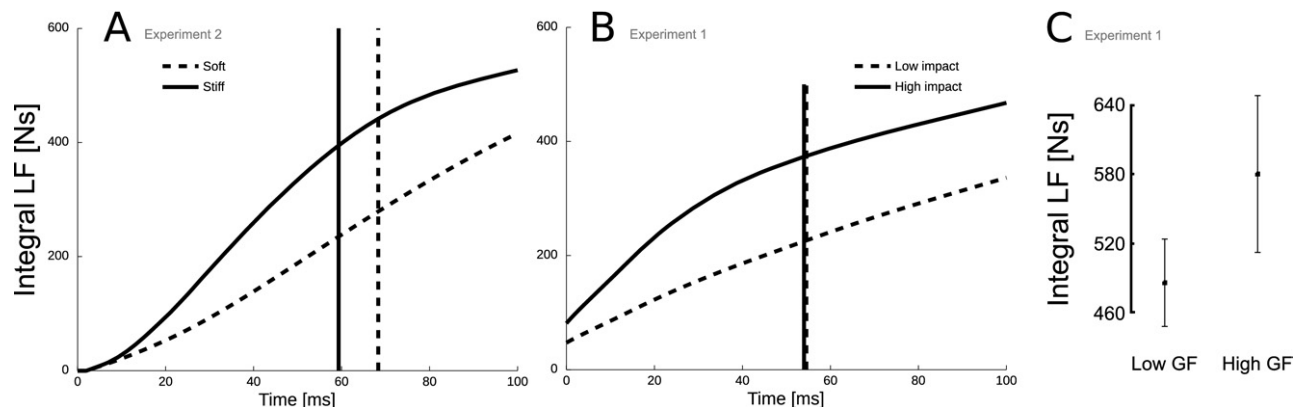


Fig. 6. (A) Evolution of the integral of load force from $t = 0$ to $t = 100$ ms after time of contact (0 ms) in Soft (dashed curve) and Stiff (solid curve) trials. The solid and dashed vertical lines are positioned at mean occurrences of grip force peaks in Stiff and Soft trials, respectively. (B) Evolution of the integral of load force from $t = 0$ to $t = 100$ ms after time of contact (0 ms) in high-impact trials (solid curve) and low-impact trials (dashed curve). The solid and dashed vertical lines are positioned at mean occurrences of grip force peaks in high-impact and low-impact trials, respectively. (C) Integral of load force 100 ms after contact for low and high grip forces at contact. Low and high grip forces were partitioned according to the median grip force for each participant.

The grip force latency is constant (65 ms) and independent of the experimental context.

DISCUSSION

Several studies have used the modulation of grip force with load force as an index of prediction in the control of voluntary movement. Various authors reported anticipatory adjustment of grip force for different forms of load force including those dependent on position, velocity and acceleration, and with impulsive as well as smoothly varying profile (Turrell et al., 1999; Flanagan et al., 2003; Nowak et al., 2004a). Here, we assessed the predictive mechanisms underlying grip force control in a task that involved active collisions with targets. The primary goal of the task was to collide with the target while stabilizing the object in hand. The object never slipped out of the grasp, which suggests a good strategy was used overall. During the initial transport phase of the movement, load force varied smoothly with acceleration while in the collision it sharply increased to values an order of magnitude larger. Results from both experiments confirmed grip-load force coupling during the transport phase but not in the collision phase. Participants pre-programmed a maximum of grip force around 65 ms after the contact in all experimental conditions, including when no real impact occurred.

In the transport phase, the tight coupling between grip and load forces demonstrates predictive control of grip force as a function of load force, whatever the direction of movement. This is in agreement with previous studies where participants adjusted their grip force according to the load force in vertical point-to-point and rhythmic movements (Flanagan and Wing, 1993, 1995; Descoins et al., 2006; Danion et al., 2009).

In the collision phase, peak grip forces were not synchronized with peak load force anymore, which is in contrast with their tight coupling during transport. Indeed, grip force increased progressively in anticipation of the occurrence of the impact and reached a maximum 65 ms after contact. This observation is in agreement with Serrien et al. (1999) who reported a ramp-like increase of grip force prior to impact, paralleled by an analogous build-up of EMG activity when opening a drawer to a predictable mechanical stop. Similarly, in their collision experiment, Turrell et al. (1999) found a maximum of grip force around 100 ms after the held object was hit by the pendulum. In the same study, the authors reported that participants synchronized the maximum of grip force with the impact only when they actively produced the collision with the pendulum in order to generate a specific amplitude swing. This provides evidence that the grip force profile after the impact contains a pre-programmed component and is not a simple reflex to the collision since it was absent in specific experimental conditions, in contrast with what is reported elsewhere when unpredictable loads were applied to a hand-held object (Johansson and Westling, 1988; Johansson et al., 1992; Nowak and Hermsdorfer, 2006). When facing collisions, the increase of EMG prior to impact and the short burst of activity after contact may reflect a mixture between anticipatory and purely reactive responses, triggered by types I and II fast adapting mechano-

receptors. Pure feedforward activity is evidenced in catch trials EMG (e.g. Fig. 4 in Johansson and Westling, 1988) and the pure “feedback” responses are elicited by the impact (Fig. 9 in Johansson and Westling, 1988). Finally, in a recent study investigating passive collisions in which blank trials were compared with impact trials, Bleyenheuft and colleagues (2009) found evidence that the late grip force component was pre-programmed. However, in their experimental design, participants performed only 15 trials among which three were blank trials at fixed position in the sequence which did not allow intra-subject analysis. Furthermore, none of these studies addressed the mechanisms underlying this motor behaviour.

Here, we found clear evidence for pre-programming of the maximum of grip force in a number of different experimental conditions involving transport of an object in two directions, impacts against real or simulated targets and with different stiffness. During catch trials in Experiment 2 (20% of the trials – 64 trials per participant), only the physical interaction with the simulated target was removed but the same grip force profile was still observed which provides very strong evidence that the peak grip force is pre-programmed.

It is interesting to ask why this peak occurred after impact and not at the time of collision, when the load force and the risk of slippage are the highest. Previous studies have shown that increments in the gain of stretch reflexes, inducing larger forces, contribute to increase the stiffness of the joint (Lacquaniti et al., 1982; Akazawa et al., 1983). Therefore, it is reasonable to assume that the larger the grip force, the stiffer the contact between the hand and the manipulandum.

To test whether there is a functional advantage to exert a moderate grip force at the time of impact, we quantified the accumulated mechanical constraints after the collision as measured by the integral of load force. Following this analysis, we found that once the peak grip force is reached, more than 70% of the destabilizing vibrations are already damped out by the skin springiness properties. We also directly showed this mechanical effect through larger integral of load force when high grip forces are applied. Indeed, grip force increases the stiffness of the contact between the hand and the manipulandum and consequently reduces the damping of the constraints induced by the collision.

Within this context, there is a clear functional advantage to rapidly absorb the vibrations (moderate grip force at contact) before increasing grip force to a maximum and stabilizing the hand against transients in the load force. Interestingly, when participants produced collisions with a pendulum, grip and load force peaks were synchronized (Turrell et al., 1999). In that specific context, participants produced movements to control the amplitude of the swings. When the hand/object stiffness increases, the system approaches the mechanics of a perfect elastic system such that the transfer of kinetic energy from the object to the pendulum could be maximized and best controlled. This is in agreement with previous results on catching (Lacquaniti et al., 1992, 1993) supporting the fact that stiffness and damping can be controlled in parallel by the Central Nervous System.

Vibrations induced by impacts may be transmitted to the upper limb and cause discomfort, pain and joint disorder.

ders (Hagberg, 2002), in addition to movement illusions. Energy transmitted to the fingers and the upper arm has a dissipative and a stored components. The first one is due to friction at the finger/object interface and the internal friction of the hand-arm system. The second component is potential and kinetic energy that can be fed back to the object. It has been shown that mostly local tissues of the fingers absorb (damp) high frequencies in the range 10–1000 Hz, which is in the range of common collisions (Dong et al., 2004). A looser grasp coincident with the impact is therefore beneficial to limit the detrimental effects of the transient. Such a feedforward control is therefore optimally suited to modulate the overall mechanical behaviour of the limb to the dynamic properties of the environment (Burdet et al., 2001; Franklin et al., 2003). Finally, this feedforward mechanism is learned through childhood (Serrien et al., 1999) and impaired in cerebellar patients, where internal models are less reliable (Nowak et al., 2004b).

In conclusion, this study extends the context of tasks in which grip force is pre-programmed by providing evidence and an explanation of feedforward mechanisms to cope with collision load forces. In the many everyday manipulations involving impacts between an object and the environment, we suggest that this constant short latency results from a compromise to maximize the damping while ensuring a safe grasp after the complex transients. The dynamics of the impact itself cannot be matched by the grip force profile but its occurrence in time is accurately predicted in order to delay the grip force peak. This strategy consisting in a modulation of grip force peak values and latencies may be adaptive in function of tasks constraints. Altogether, this suggests that the central nervous system controls hand impedance through grip force to account for the dynamics of the task. This study provides novel insights about how the brain coordinates grip force in manipulations involving transport and impact loads.

Acknowledgments—This research was supported by grants from Prodex, OSTC (Belgian Federal Office for Scientific, Technical and Cultural affairs), FSR and ESA, ESTEC Contract 14725/00/NLJS to JLT, from the UK Medical Research Council to AMW, and EU IST to AMW and RMB and by a Grant from the Biotechnology and Biological Sciences Research Council (BB/E009174/1), from the National Science Foundation (BSC 0726685) (both to JD). The authors declare no competing interests.

REFERENCES

- Akazawa K, Milner TE, Stein RB (1983) Modulation of reflex EMG and stiffness in response to stretch of human finger muscle. *J Neurophysiol* 49:16–27.
- Bleyenheuff Y, Lefèvre P, Thonnard JL (2009) Predictive mechanisms control grip force after impact in self-triggered perturbations. *J Mot Behav* 41(5):411–417.
- Burdet E, Osu R, Franklin DW, Milner TE, Kawato M (2001) The central nervous system stabilizes unstable dynamics by learning optimal impedance. *Nature* 414:446–449.
- Danion F, Descoins M, Bootsma RJ (2009) When the fingers need to act faster than the arm: coordination between grip force and load force during oscillation of a hand-held object. *Exp Brain Res* 193:85–94.
- Delevoeye-Turrell YN, Li FX, Wing AM (2003) Efficiency of grip force adjustments for impulsive loading during imposed and actively produced collisions. *Q J Exp Psychol A* 56:1113–1128.
- Descoins M, Danion F, Bootsma RJ (2006) Predictive control of grip force when moving object with an elastic load applied on the arm. *Exp Brain Res* 172:331–342.
- Dong RG, Schopper AW, McDowell TW, Welcome DE, Wu JZ, Smutz WP, et al (2004) Vibration energy absorption (VEA) in human fingers-hand-arm system. *Med Eng Phys* 26(6):483–492.
- Flanagan JR, Tresilian J, Wing AM (1993) Coupling of grip force and load force during arm movements with grasped objects. *Neurosci Lett* 152:53–56.
- Flanagan JR, Vetter P, Johansson RS, Wolpert DM (2003) Prediction precedes control in motor learning. *Curr Biol* 13:146–150.
- Flanagan JR, Wing AM (1993) Modulation of grip force with load force during point-to-point arm movements. *Exp Brain Res* 95:131–143.
- Flanagan JR, Wing AM (1995) The stability of precision grip forces during cyclic arm movements with a hand-held load. *Exp Brain Res* 105:455–464.
- Flanagan JR, Wing AM (1997) The role of internal models in motion planning and control: evidence from grip force adjustments during movements of hand-held loads. *J Neurosci* 17:1519–1528.
- Franklin DW, Burdet E, Osu R, Kawato M, Milner TE (2003) Functional significance of stiffness in adaptation of multijoint arm movements to stable and unstable dynamics. *Exp Brain Res* 151:145–157.
- Hagberg M (2002) Clinical assessment of musculoskeletal disorders in workers exposed to hand-arm vibration. *Int Arch Occup Environ Health* 2(75):97–105.
- Johansson RS, Riso R, Hager C, Backstrom L (1992) Somatosensory control of precision grip during unpredictable pulling loads. I. Changes in load force amplitude. *Exp Brain Res* 89:181–191.
- Johansson RS, Westling G (1988) Programmed and triggered actions to rapid load changes during precision grip. *Exp Brain Res* 71:72–86.
- Lacquaniti F, Borghese NA, Carrozzo M (1992) Internal models of limb geometry in the control of hand compliance. *J Neurosci* 12:1750–1762.
- Lacquaniti F, Carrozzo M, Borghese NA (1993) Time-varying mechanical behavior of multijointed arm in man. *J Neurophysiol* 69:1443–1464.
- Lacquaniti F, Licata F, Soechting JF (1982) The mechanical behavior of the human forearm in response to transient perturbations. *Biol Cybern* 44:35–46.
- Nowak DA, Hermsdorfer J (2006) Predictive and reactive control of grasping forces: on the role of the basal ganglia and sensory feedback. *Exp Brain Res* 173:650–660.
- Nowak DA, Hermsdorfer J, Schneider E, Glasauer S (2004a) Moving objects in a rotating environment: rapid prediction of Coriolis and centrifugal force perturbations. *Exp Brain Res* 157:241–254.
- Nowak DA, Hermsdorfer J, Rost K, Timmann D, Topka H (2004b) Predictive and reactive finger force control during catching in cerebellar degeneration. *Cerebellum* 3:227–235.
- Serrien DJ, Kaluzny P, Wicki U, Wiesendanger M (1999) Grip force adjustments induced by predictable load perturbations during a manipulative task. *Exp Brain Res* 124:100–106.
- Turrell YN, Li FX, Wing AM (1999) Grip force dynamics in the approach to a collision. *Exp Brain Res* 128:86–91.
- White O, Penta M, Thonnard JL (2008) A new device to measure the three dimensional forces and torques in precision grip tasks. *J Med Eng Technol* 33(3):245–248.
- Wing AM (1996) Anticipatory control of grip force in rapid arm movement. In: *Hand and brain: the neurophysiology and psychology of hand movements* (Wing AM, Haggard P, Flanagan JR, eds), pp 301–324. San Diego: Academic.